J. Appl. Comput. Mech., 6(SI) (2020) 1314-1323
DOI: 10.22055/JACM.2020.33959.2314

ISSN: 2383-4536
jacm.scu.ac.ir

Shahid Chamran University of Ahvaz

Journal of Applied and Computational Mechanics

Research Paper

A Novel Quadrilateral Element for Dynamic Response of Plate Structures Subjected to Blast Loading

Hoang Lan Ton-That

Faculty of Civil Engineering, Ho Chi Minh City University of Architecture, 196 Pasteur Street, District 3, Ho Chi Minh City, Viet Nam

Received June 12 2020; Revised August 03 2020; Accepted for publication August 03 2020.
Corresponding author: Hoang Lan Ton-That (lan.tonthathoang@uah.edu.vn)

Abstract. We study the dynamic response of plate structures subjected to blast loading. This load is introduced in dynamically excited form over time. Two assumptions are given to ensure the physical properties of dynamic problems. The plate structures are studied its response under explosion. The governing equation with respect to the motion is solved by using a novel quadrilateral element SQ4T related to the twice interpolation strategy (TIS) and the average acceleration method of Newmark's family. Our solutions are compared with reference solutions to confirm the accuracy of the proposed element.

Keywords: Dynamic analysis, Plate, Blast loading, First-order shear deformation theory, Twice interpolation strategy.

1. Introduction

As we know that the modelling of blast pressure on structures has been mentioned for a long time. In [1] the spherical blast waves were introduced by the numerical way. The strong-shock, point-source solution and spherical isothermal distributions were used as initial conditions for a numerical integration of the differential equations of gas motion in Lagrangean form. The von Neumann-Richtmyer artificial viscosity was employed to avoid shock discontinuities and the analytical approximations to the numerical results are provided. Within [2], the author recommended to develop research on the explosion of structures, mainly from the early twentieth century. Major contributions in the areas of measurement, analysis and prediction were discussed. Conventional high explosive dynamic loads have been tested, as well as the effects of liquid fuels, dust, gases, vapors and fuel/air explosions. Subjects included tunnel explosions, underground and underwater explosions, pressure measurements and explosion simulations. Explosive effects on all structures have been summarized, including estimates of residual strength. Furthermore, the theory of stress waves and the explosion with its effects within a medium in general terms as well as the behavior of shaped charges were introduced in [3]. The expressions shown for the blast loading allowed to predict the impact field for any distance and obviously this load is described equivalent to TNT. The interaction between the blast wave and a stationary target surface was also studied in [4]. One different way was given in which each plate element was considered as a single degree of freedom system in the dynamic analysis [5]. The design of plate structures subjected to blast loads require a detailed understanding of blast phenomena and the dynamic response of various structural members. More details and reviews of the literature related to blast loading for plate structures may be found in [6-13]. There were other documents of Rabczuk et al. [14-16] in which explosives were clearly modelled, leading to very good results, but the goal of this paper is to simplify the problem, although the results may not be as good as theirs. Due to the finite element analysis, the first-order shear deformation theory (FSDT) is simple to implement and applied for plate structures but the shear correction factors are used to achieve the accuracy of solutions. Hence, the standard finite element code associated with the FSDT are showing believable results and easy operation. The quadrilateral elements are usually used with respect to their better performance than other elements. The quadrilateral element related to thin plates will be treated by using shear correction factors [17-19].

The main of current study is to determine the dynamic response of the plates under blast loads based on a novel quadrilateral element SQ4T related to the twice interpolation strategy (TIS) [20-22]. The TIS with several desirable characteristics are used to evaluate all parts of element stiffness matrices. The negative phase of exponential form in time is used to describe the pressure of explosion. The plate is modeled as a system with multi degrees of freedom and the governing equation with respect to the motion can be solved by using the SQ4T elements associated with the average acceleration method of Newmark's family. The rest of this paper is structured as follows. We briefly present in section 2 the formulation of blast loading and of the SQ4T element based on the TIS. Section 3 shows the numerical results and some discussions related to the robustness and accuracy of the SQ4T elements. Finally, some conclusions drawn from the study are presented in the last section.

2. Formulation for Dynamic Response

2.1 The first-order shear deformation theory (FSDT)

The first-order shear deformation theory (FSDT) for plates includes the effect of transverse shear deformations. In the FSDT, the normal to the undeformed middle plane of the plate remain straight, but not normal to the deformed middle surface.

Published online: August 28 2020

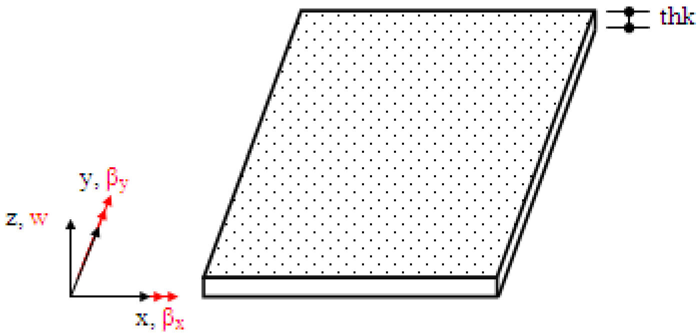

Fig. 1. A plate with positive definition of displacements, rotations.

The displacements can be presented in form of the first-order shear deformation theory (FSDT) [23] as below

$$\begin{aligned} u(x,y,z) &= z\beta_x \\ v(x,y,z) &= z\beta_y \\ w(x,y,z) &= w_0 \end{aligned} \tag{1}$$

with three translational displacements, namely u, v, and w, are in the x-, y-, and z- directions; w_0 correspond to the displacement in the z- direction of the middle plane; and β_x and β_y are respectively the rotation of the mid-plane about x- and y- axis with positive directions defined in Figure 1.
The bending strains are obtained as

$$\boldsymbol{\varepsilon} = \begin{Bmatrix} \varepsilon_x \\ \varepsilon_y \\ \gamma_{xy} \end{Bmatrix} = \begin{Bmatrix} u_{,x} \\ v_{,y} \\ u_{,y} + v_{,x} \end{Bmatrix} \tag{2}$$

while the transverse shear deformations are obtained as

$$\boldsymbol{\gamma} = \begin{Bmatrix} \gamma_{xz} \\ \gamma_{yz} \end{Bmatrix} = \begin{Bmatrix} \beta_x + w_{,x} \\ \beta_y + w_{,y} \end{Bmatrix} \tag{3}$$

The linear elastic stress-strain relations in bending are defined for a homogeneous, isotropic material as

$$\boldsymbol{\sigma} = \mathrm{D}_b \boldsymbol{\varepsilon} \tag{4}$$

where $\mathbf{D}_b$ is defined as

$$\mathbf{D}_b = \frac{E}{1-\nu^2} \begin{bmatrix} 1 & \nu & 0 \\ \nu & 1 & 0 \\ 0 & 0 & \frac{1-\nu}{2} \end{bmatrix} \tag{5}$$

while the linear elastic stress-strain relations in transverse shear are defined as

$$\boldsymbol{\tau} = \mathrm{D}_s \boldsymbol{\gamma} \tag{6}$$

with

$$\mathbf{D}_s = \frac{E}{2(1+\nu)} \begin{bmatrix} 1 & 0 \\ 0 & 1 \end{bmatrix} \tag{7}$$

2.2 The twice-interpolation strategy (TIS)

A point $\mathbf{x}_C$ is considered in a quadrilateral element that has four nodes, namely i, j, k and m, as depicted in Figure 2. We indicate by S_i, S_j, S_k and S_m elements that share these four nodes. All nodes of elements S_i, S_j, S_k and S_m are called the supporting nodes of the point $\mathbf{x}_C$. Because of this reason, the standard FEM support domain is always smaller than the support domain of point $\mathbf{x}_C$ respectively. The trial solution at this point can be presented

$$\tilde{u}(x) = \sum_{l=1}^{n_{sp}} \tilde{N}_l(x) d_l = \tilde{N}(x)\mathbf{d} \tag{8}$$

In Equation (8), the shape function $\tilde{N}_l$ based on the twice-interpolation strategy is given

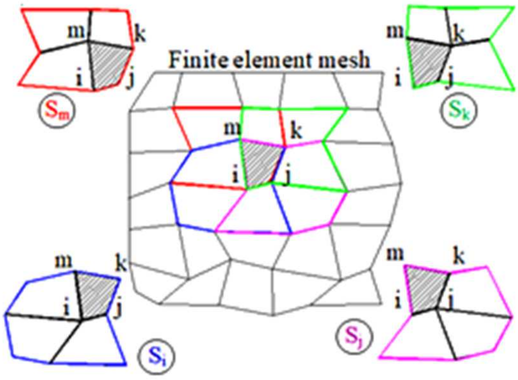

Fig. 1. The twice interpolation strategy and the 2D support domain

$$\begin{aligned}\tilde{N}_I &= \phi_i N_I^{[i]} + \phi_j N_I^{[j]} + \phi_k N_I^{[k]} + \phi_m N_I^{[m]} + \phi_{ix}\bar{N}_{I,x}^{[i]} + \phi_{jx}\bar{N}_{I,x}^{[j]} + \\ &+\phi_{kx}\bar{N}_{I,x}^{[k]} + \phi_{mx}\bar{N}_{I,x}^{[m]} + \phi_{iy}\bar{N}_{I,y}^{[i]} + \phi_{jy}\bar{N}_{I,y}^{[j]} + \phi_{ky}\bar{N}_{I,y}^{[k]} + \phi_{my}\bar{N}_{I,y}^{[m]}\end{aligned} \tag{9}$$

with $N_I^{[i]}$ is called the shape function related to node i, and n_{sp} is the number of nodes in the support domain with respect to the point $\mathbf{x}_C$, while d_I indicates the nodal displacement vector.
The average derivatives of the shape function at node i are formulated as follows with note that the setup is completely similar for the other nodes

$$\bar{N}_{I,x}^{[i]} = \sum_{el\in S_i}(\omega_{el} N_{I,x}^{[i][el]}) \qquad \bar{N}_{I,y}^{[i]} = \sum_{el\in S_i}(\omega_{el} N_{I,y}^{[i][el]}) \tag{10}$$

In Equation (10), the term $N_{I,x}^{[i][el]}$ related to element el is called the derivative of $N_I^{[i]}$, and the weight function, namely ω_{el}, of element $el \in S_i$ is given

$$\omega_{el} = \Lambda_{el} / \sum_{\bar{el}\in S_i}\Lambda_{\bar{el}} \qquad \text{with} \quad el \in S_i \tag{11}$$

in which Λ_{el} is the area of the element el. In Equation (9), three functions ϕ_i, ϕ_{ix} and ϕ_{iy} with respect to node i must satisfy the below conditions

$$\begin{gathered}\phi_i(\mathbf{x}_s) = \delta_{is} \qquad \phi_{i,x}(\mathbf{x}_s) = 0 \qquad \phi_{i,y}(\mathbf{x}_s) = 0 \qquad \phi_{ix}(\mathbf{x}_s) = 0 \qquad \phi_{ix,x}(\mathbf{x}_s) = \delta_{is} \qquad \phi_{ix,y}(\mathbf{x}_s) = 0 \\ \phi_{iy}(\mathbf{x}_s) = 0 \qquad \phi_{iy,x}(\mathbf{x}_s) = 0 \qquad \phi_{iy,y}(\mathbf{x}_s) = \delta_{is}\end{gathered} \tag{12}$$

with s is taken from four characters i, j, k, m respectively.

$$\delta_{is} = \begin{cases}1 & \text{if} \quad i = s \\ 0 & \text{if} \quad i \neq s\end{cases} \tag{13}$$

These conditions must be applied in the same way for ϕ_j, ϕ_k, ϕ_m, ϕ_{jx}, ϕ_{kx}, ϕ_{mx}, ϕ_{jy}, ϕ_{ky} and ϕ_{my}. There basis functions ϕ_i, ϕ_{ix} and ϕ_{iy} for the quadrilateral element are presented

$$\begin{aligned}&\phi_i = L_i - L_iL_j^2 - L_iL_k^2 - L_iL_m^2 + L_i^2L_j + L_i^2L_k + L_i^2L_m \\ &\quad \phi_{ix} = -x_i(L_i^2L_m + 0.5L_iL_mL_j + 0.5L_iL_mL_k + L_i^2L_k + 0.5L_iL_kL_j + 0.5L_iL_kL_m + L_i^2L_j + 0.5L_iL_jL_k + 0.5L_iL_jL_m) + \\ &\quad +x_m(L_i^2L_m + 0.5L_iL_mL_j + 0.5L_iL_mL_k) + x_k(L_i^2L_k + 0.5L_iL_kL_j + 0.5L_iL_kL_m) + x_j(L_i^2L_j + 0.5L_iL_jL_k + 0.5L_iL_jL_m) \\ &\quad \phi_{iy} = -y_i(L_i^2L_m + 0.5L_iL_mL_j + 0.5L_iL_mL_k + L_i^2L_k + 0.5L_iL_kL_j + 0.5L_iL_kL_m + L_i^2L_j + 0.5L_iL_jL_k + 0.5L_iL_jL_m) + \\ &\quad +y_m(L_i^2L_m + 0.5L_iL_mL_j + 0.5L_iL_mL_k) + y_k(L_i^2L_k + 0.5L_iL_kL_j + 0.5L_iL_kL_m) + y_j(L_i^2L_j + 0.5L_iL_jL_k + 0.5L_iL_jL_m)\end{aligned} \tag{14}$$

Other functions can be established in the same way by a circulatory permutation of the index i, j, k and m. In the other hand, the area coordinates L_i, L_j, L_k and L_m are of point $\mathbf{x}_C$ in the domain that related to the four-node element as seen [24-26]. These polynomial shape functions satisfy the properties of the partition of unity as well as the properties of the Kronecker delta function.

2.3 The SQ4T element and its application

With three degrees of freedom for one node, the bending strains at point $\mathbf{x}_C$ can be achieved as below

$$\varepsilon(\mathbf{x}_C) = \mathbf{B}_b(\mathbf{x}_C)\mathbf{q} \tag{15}$$

where

$$\mathbf{q}_i = \begin{bmatrix} w_i & \beta_{xi} & \beta_{yi}\end{bmatrix}^T \tag{16}$$

$$\mathbf{B}_b(\mathbf{x}_C)=\begin{bmatrix} 0 & \tilde{N}_{1,x} & 0 & \dots & 0 & \tilde{N}_{n_{sp},x} & 0 \\ 0 & 0 & \tilde{N}_{1,y} & \dots & 0 & 0 & \tilde{N}_{n_{sp},y} \\ 0 & \tilde{N}_{1,y} & \tilde{N}_{1,x} & \dots & 0 & \tilde{N}_{n_{sp},y} & \tilde{N}_{n_{sp},x} \end{bmatrix}_{3\times 3n_{sp}} \tag{17}$$

with n_{sp} is the number of nodes in the support domain with respect to $\mathbf{x}_C$.
The shear strains are also expressed by

$$\gamma(\mathbf{x}_C)=\mathbf{B}_s(\mathbf{x}_C)\mathbf{q} \tag{18}$$

where

$$\mathbf{B}_s(\mathbf{x}_C)=\begin{bmatrix} \tilde{N}_{1,x} & \tilde{N}_1 & 0 & \dots & \tilde{N}_{n_{sp},x} & \tilde{N}_{n_{sp}} & 0 \\ \tilde{N}_{1,y} & 0 & \tilde{N}_1 & \dots & \tilde{N}_{n_{sp},y} & 0 & \tilde{N}_{n_{sp}} \end{bmatrix}_{2\times 3n_{sp}} \tag{19}$$

The stiffness matrix of SQ4T element is established

$$K^{el}=K_b+K_s=\int_\Omega \mathbf{B}_b^T\mathbf{D}_b\mathbf{B}_b d\Omega+\int_\Omega \mathbf{B}_s^T\mathbf{D}_s\mathbf{B}_s d\Omega \tag{20}$$

The element mass matrix $\mathbf{M}^{el}$ is obtained in a similar way with [27]. Finally, the equations of motion of system can be expressed by

$$\mathbf{M}\ddot{\mathbf{q}}(t)+\mathbf{C}\dot{\mathbf{q}}(t)+\mathbf{K}\mathbf{q}(t)=\mathbf{P}(t) \tag{21}$$

with Rayleigh damping

$$\mathbf{C}=\alpha_1\mathbf{M}+\alpha_2\mathbf{K} \tag{22}$$

$$\alpha_1=\alpha_2\omega_1\omega_2 \quad \text{and} \quad \alpha_2=\frac{2\xi}{\omega_1+\omega_2} \tag{23}$$

where α_1,α_2 are real scalars; ω_1,ω_2 are two first frequencies in free vibration analysis; ξ is damping ratio and the average acceleration method (γ = 1/2 and β = 1/4) of Newmark's family which is unconditionally stable if γ ≥ 1/2 and β ≥ 1/4(γ + 0.5)^2 will be used to solve (21). The procedure will be established with the following algorithm:

a. *Initial calculations*
   a1. $\ddot{\mathbf{q}}_o=\dfrac{\mathbf{P}_o-\mathbf{C}\dot{\mathbf{q}}_o-\mathbf{K}\mathbf{q}_o}{\mathbf{M}}$
   a2. Select Δt *(Note that: based on the time which the pressure of explosion returns to equal with atmospheric pressure, the time step can be predicted)*
   a3. $\hat{\mathbf{K}}=\mathbf{K}+\dfrac{\gamma}{\beta\Delta t}\mathbf{C}+\dfrac{1}{\beta(\Delta t)^2}\mathbf{M}$
   a4. $\delta_1=\dfrac{1}{\beta\Delta t}\mathbf{M}+\dfrac{\gamma}{\beta}\mathbf{C}$ and $\delta_2=\dfrac{1}{2\beta}\mathbf{M}+\Delta t\left(\dfrac{\gamma}{2\beta}-1\right)\mathbf{C}$
b. *Calculations for each time step I*
   b1. $\Delta\hat{\mathbf{P}}_i=\Delta\mathbf{P}_i+\delta_1\dot{\mathbf{q}}_i+\delta_2\ddot{\mathbf{q}}_i$ (24)
   b2. $\Delta\mathbf{q}_i=\dfrac{\Delta\hat{\mathbf{P}}_i}{\hat{\mathbf{K}}}$
   b3. $\Delta\dot{\mathbf{q}}_i=\dfrac{\gamma}{\beta\Delta t}\Delta\mathbf{q}_i-\dfrac{\gamma}{\beta}\dot{\mathbf{q}}_i+\Delta t\left(1-\dfrac{\gamma}{2\beta}\right)\ddot{\mathbf{q}}_i$
   b4. $\Delta\ddot{\mathbf{q}}_i=\dfrac{1}{\beta(\Delta t)^2}\Delta\mathbf{q}_i-\dfrac{1}{\beta\Delta t}\dot{\mathbf{q}}_i-\dfrac{1}{2\beta}\ddot{\mathbf{q}}_i$
   b5. $\mathbf{q}_{i+1}=\mathbf{q}_i+\Delta\mathbf{q}_i$, $\dot{\mathbf{q}}_{i+1}=\dot{\mathbf{q}}_i+\Delta\dot{\mathbf{q}}_i$, $\ddot{\mathbf{q}}_{i+1}=\ddot{\mathbf{q}}_i+\Delta\ddot{\mathbf{q}}_i$
c. *Repetition for the next time step. Replace i by i+1 and implement steps b1 to b5 for the next time step.*

2.4 Properties of the blast loading

By following [5], two assumptions with respect to the dynamic response of plate structures as well as the blast are given as: *i)* the common "hemispherical" blast scenarios is used for the form of wave; *ii)* explosions are "far enough" to ensure the physical root of dynamic analysis. Estimations of peak overpressure due to spherical blast related to the scaled distance $Z=R/W^{(1/3)}$ is presented in [1]

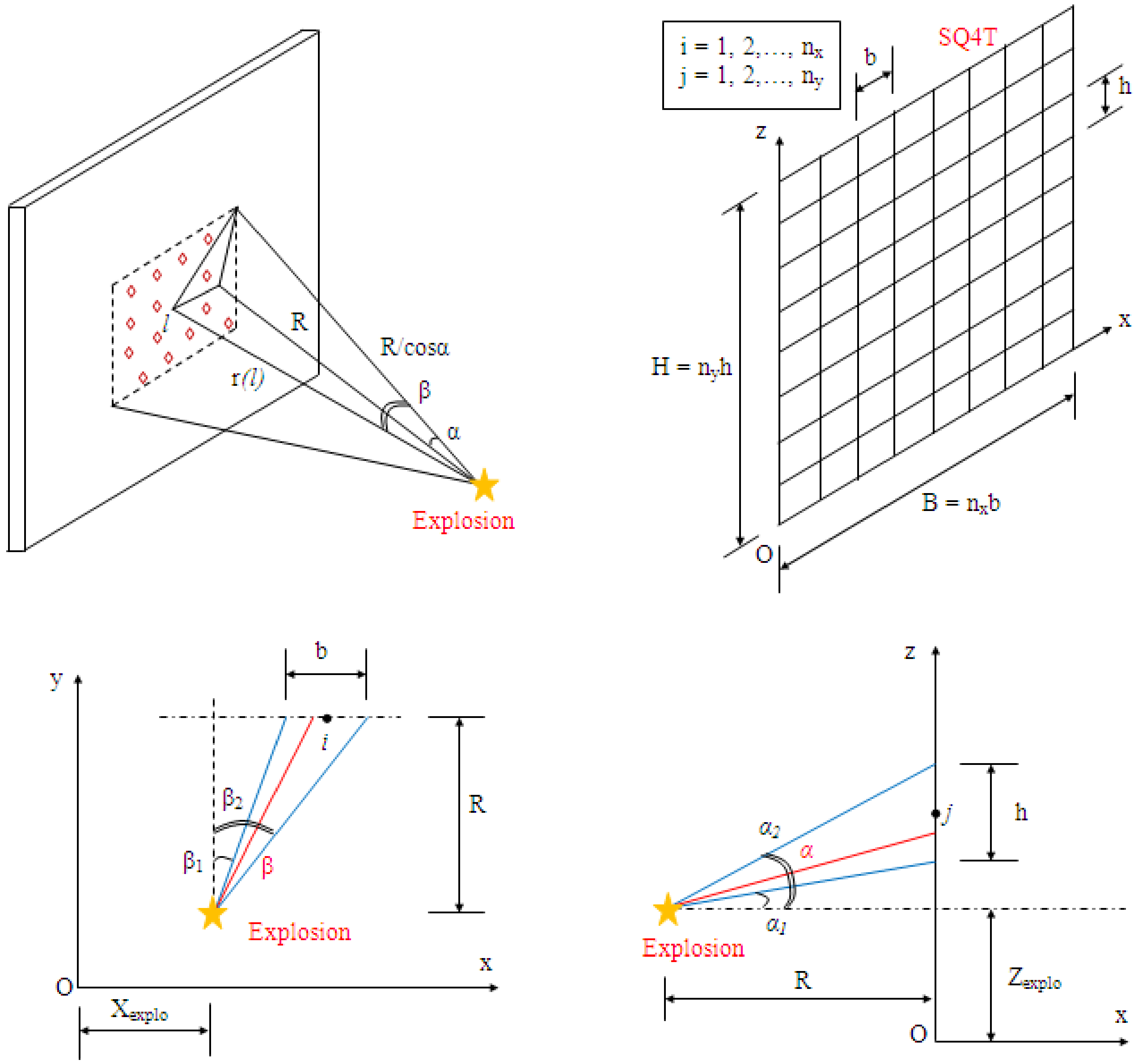

Fig. 3. The plate and explosion are described with various parameters.

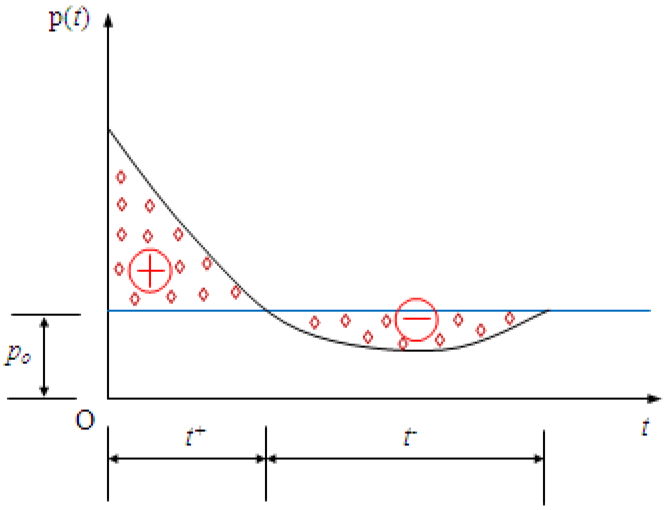

Fig. 4. The variation of blast loading.

$$p_s = \frac{670}{Z^3} + 100 \quad (\mathrm{kN/m^2}) \quad \text{if} \quad (p_s > 1000 \quad \mathrm{kN/m^2})$$
$$\text{and} \quad p_s = \frac{97.5}{Z} + \frac{145.5}{Z^2} + \frac{585}{Z^3} - 1.9 \quad (\mathrm{kN/m^2}) \quad \text{if} \quad (10 \quad \mathrm{kN/m^2} < p_s < 1000 \quad \mathrm{kN/m^2}) \tag{25}$$

with the stand-off distance (m) is named R; the charge weight of the blast related to TNT equivalence (kg) is called W. The variation of this pressure is presented as follows [2]

$$p(t) = p_o + p_s\left(1 - \frac{t}{T_s}\right)e^{-\gamma\frac{t}{T_s}} \qquad p_o = 101 \quad (\mathrm{kN/m^2}) \tag{26}$$

in which the pressure $p(t)$ in time t is used and γ is called the parameter controlling the rate of wave amplitude dissipation; T_s is the time which the pressure is equal to atmospheric pressure p_o.
These values of γ and T_s are given as [4, 28]

$$\gamma = Z^2 - 3.7\,Z + 4.2 \qquad T_s = W^{(1/3)}10^{\left[-2.75 + 0.27\log\left(R/W^{(1/3)}\right)\right]} \tag{27}$$

Furthermore, the C_r which is called the coefficient for the reflected over-pressure is introduced in [28]

$$C_r = 3\left(\frac{p_{s\max}}{p_o}\right)^{1/4} \tag{28}$$

with $p_{s\max}$ is the peak static pressure.
The pressure based on blast is thus presented related to C_r as

$$p(t) = p_o + C_r p_s\left(1 - \frac{t}{T_s}\right)e^{-\gamma\frac{t}{T_s}} \tag{29}$$

Finally, the blast loading on each node of finite elements for a plate as shown in Figure 3 is presented as

$$P_{ij} = \int_{\alpha_i}^{\alpha_j}\int_{\beta_i}^{\beta_j} p(t)\,d\alpha\,d\beta \tag{30}$$

Figure 4 presents the variation of blast loading with positive phase and negative phase. Based on these databases, the response of plate structures under blast loading are calculated.

3. Solutions and Discussions

The SQ4T element will be used through numerical examples. The value 5/6 is used for shear correction factors as well as SI units are used for all examples in this paper.

3.1 A study of the convergence

The static bending and free vibration analysis of plate are considered to verify the convergence of present code with SQ4T elements. The plate has B = 1m, H = 3m, thickness thk = 0.1m, 0.15m, 0.2m & 0.25m, and its material properties: E = $2.7\text{x}10^7$ kN/m^2, ρ = 25 kN/m^3, ν = 0.17 as shown in Figure 5a. Under uniform load p = 1 kN/m^2, the deflections of central top point related to various thickness t are achieved by using proposed elements and they are good agreement with the solutions using Sap2000 software as shown in Figure 5b and Table 1.

With two values 0.1m and 0.15m of thickness thk, the natural periods of the first two modes of this plate are presented in Table 2 and compared with the results of BlastShell code and Sap2000 [5] as given in Figure 5c-f. The errors between them may be negligible when increasing the number of elements.

3.2 A rectangular plate with clamped at bottom edge under blast loading

In this section, the above plate will be studied under blast loading. The damping ratio ξ is equal to 0.05. The parameters related to this example are R = 10m, W = 625 kg, Z_{explo} = 1.5m and X_{explo} = 0.5m. The full plate is calculated with clamped at bottom edge as shown in Figure 6a. The dynamic response of this structure subjected to blast loading is solved and the deflection of central point is compared with other results based on finite element code BlastShell [5] as shown in Figure 6b.

Next, we also study the effect of the distance R on the central deflection. Three values 8m, 10m and 12m of R are used to calculate the dynamic reponse of plate through the curves of the central deflection as shown in Figure 7a. It is shown that the maximum central deflection decreases as the value of R increases. Finally, the effect of the W is also presented. With three values W = 400kg, 500kg and 600kg, the dynamic reponse of plate through the variation of the central deflection is also plotted in Figure 7b. It is again shown that the central deflection decreases as the value of W decreases, respectively.

3.3 A square plate with clamped at all edges under blast loading

The deflection of central point – time curve of the blast loaded square plate will be obtained in this section. The plate has B = H = 2m, thickness thk = 0.5m and its material properties: E = $7\text{x}10^7$ kN/m^2, ρ = 2700 kg/m^3, ν = 0.3 as shown in Figure 8a. Furthermore, the blast load parameters are taken as $p_{s\max}$ = 28.906 kN/m^2, γ = 0.35 and T_s = 0.0018. Figure 8b shows the present result and its error is small enough when compared with the other results found in the literature [12] based on the differential quadrature method (DQM), Ansys software (ANSYS) and analytical solution (THEORY).

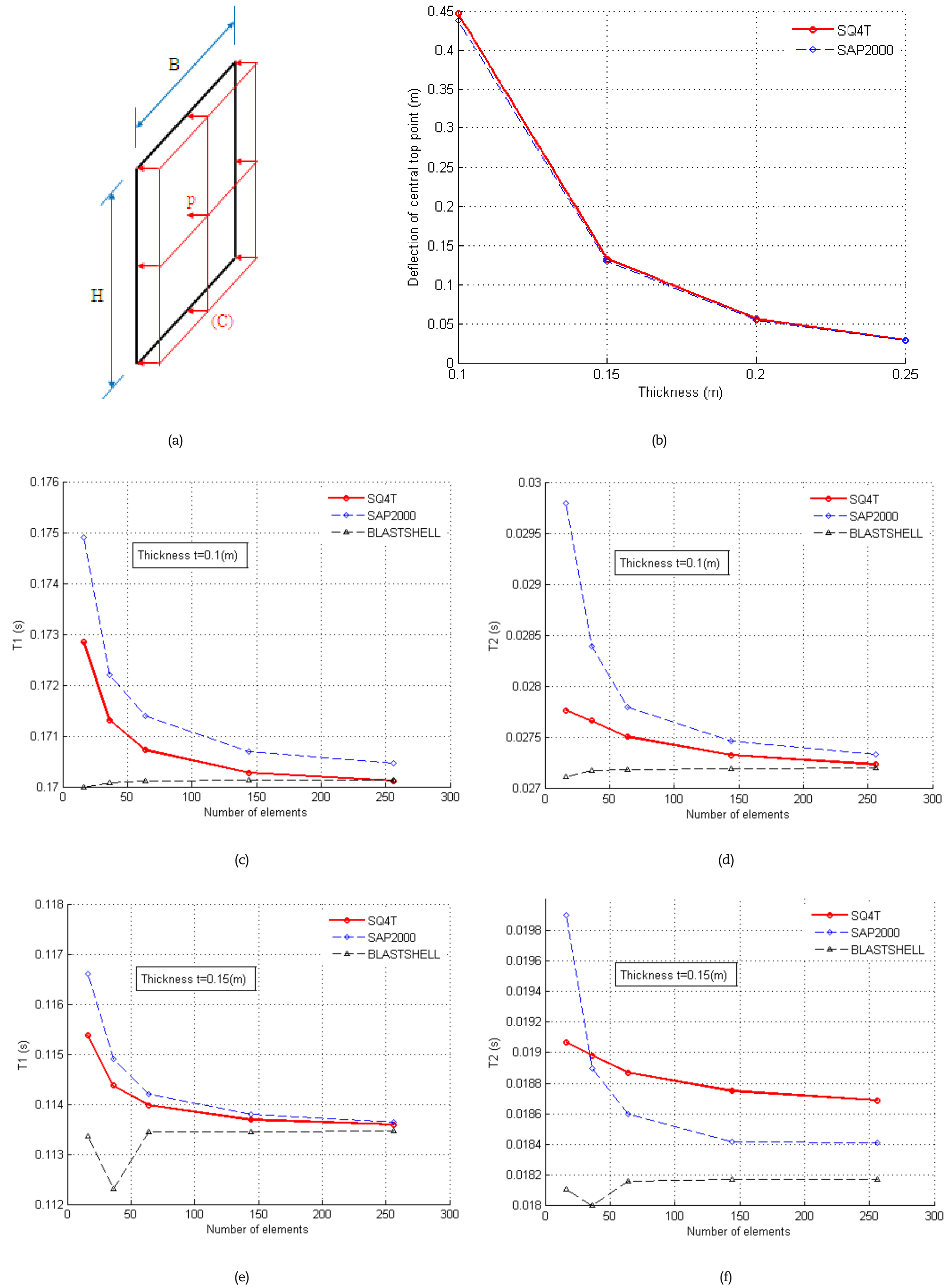

Fig. 5. (a) The geometry, (b) The comparison of the deflections of central top point, (c) The period T_1 with thk =0.1m, (d) The period T_2 with thk = 0.1m, (e) The period T_1 with thk = 0.15m and (f) The period T_2 with thk =0.15m

Table 1. The comparison of the central top point's deflection.

Deflection (m)	Thickness thk of plate (m)			
	0.1	0.15	0.2	0.25
SAP2000	0.43725	0.12956	0.05466	0.02798
SQ4T	0.44636	0.13256	0.05609	0.02881

Table 2. The comparison of the natural periods.

Periods	Thickness thk = 0.1(m)					
Mesh	SAP2000		BlastShell		SQ4T	
	T_1 (s)	T_2 (s)	T_1 (s)	T_2 (s)	T_1 (s)	T_2 (s)
4x4	0.17490	0.02980	0.17000	0.02712	0.17285	0.02777
6x6	0.17220	0.02840	0.17008	0.02718	0.17131	0.02767
8x8	0.17140	0.02780	0.17011	0.02719	0.17072	0.02751
12x12	0.17069	0.02747	0.17013	0.02720	0.17028	0.02733
16x16	0.17046	0.02734	0.17014	0.02721	0.17012	0.02724
Periods	Thickness thk = 0.15(m)					
Mesh	SAP2000		BlastShell		SQ4T	
	T_1 (s)	T_2 (s)	T_1 (s)	T_2 (s)	T_1 (s)	T_2 (s)
4x4	0.11660	0.01990	0.11336	0.01811	0.11538	0.01907
6x6	0.11490	0.01890	0.11230	0.01800	0.11437	0.01898
8x8	0.11420	0.01860	0.11344	0.01816	0.11398	0.01887
12x12	0.11380	0.01842	0.11345	0.01817	0.11369	0.01875
16x16	0.11364	0.01841	0.11346	0.01817	0.11359	0.01869

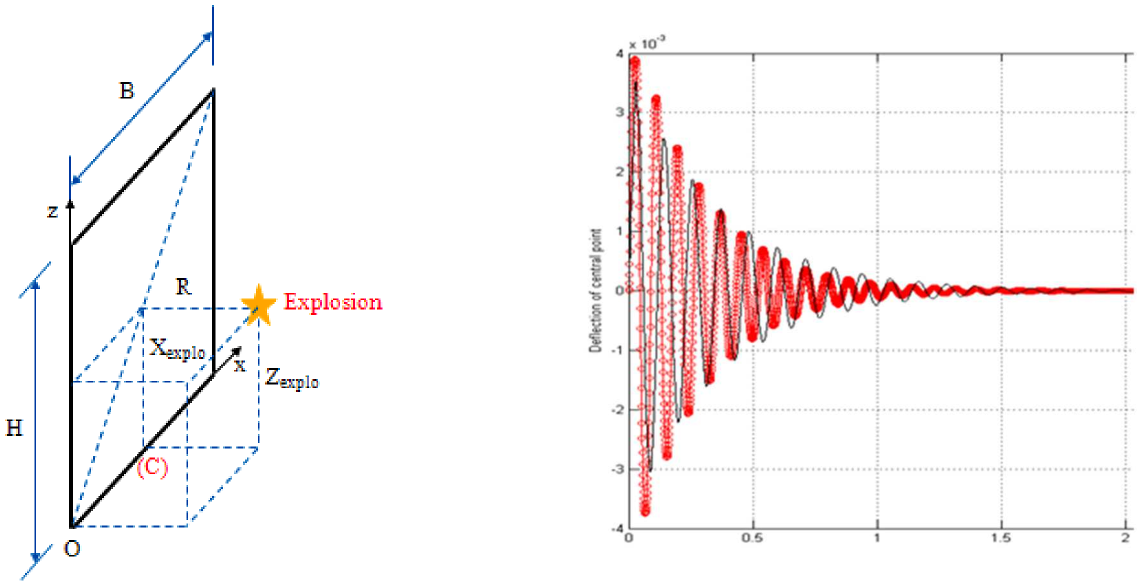

(a) (b)

Fig. 6. (a) The plate with clamped (C) at bottom edge subjected to blast loading, (b) The comparison of the deflection of central point (red for SQ4T and black for BLASTSHELL).

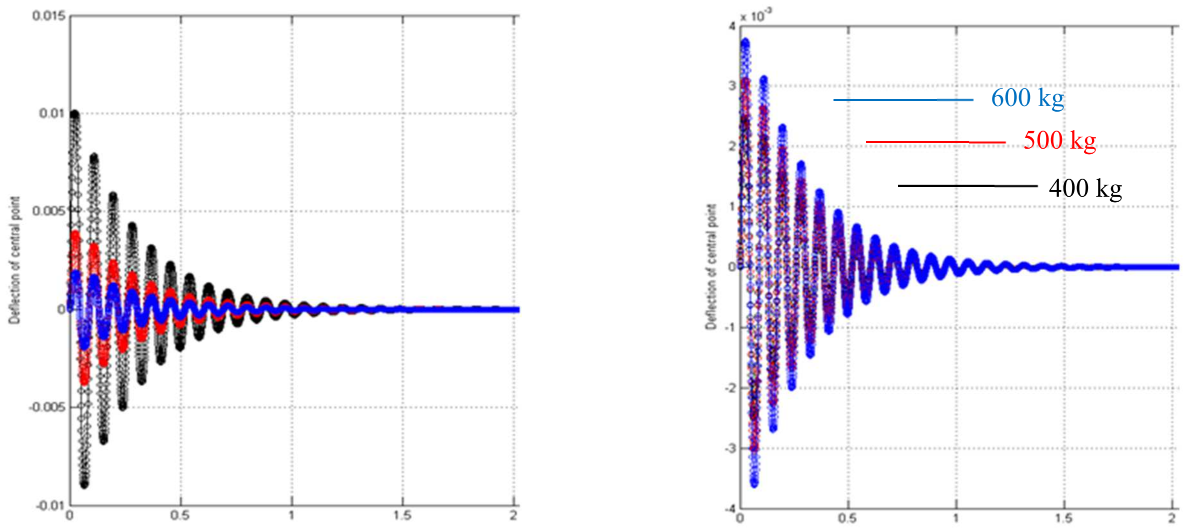

(a) (b)

Fig. 7. (a) The effect of R on the deflection of central point (R = 8m _black, R = 10m _red & R = 12m _blue) ; (b) The effect of W on the deflection of central point (W = 400kg _black, W = 500kg _red & W = 600kg _blue).

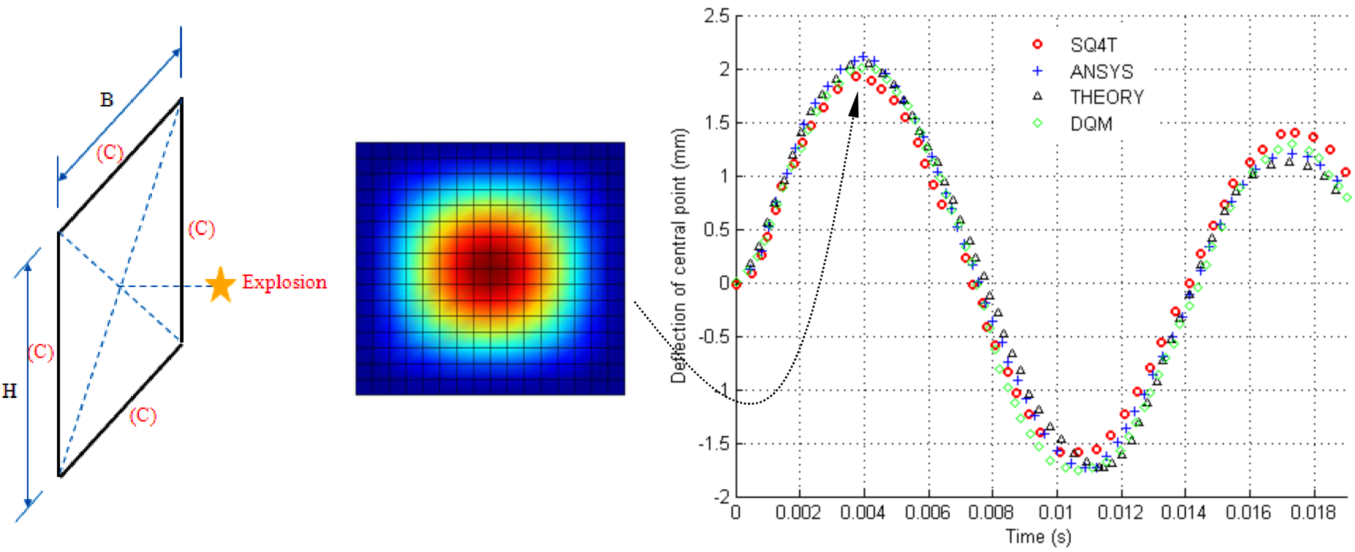

(a) (b)

Fig. 8. (a) The plate with clamped (C) at all edges subjected to blast loading, (b) The comparison of the deflection of central point.

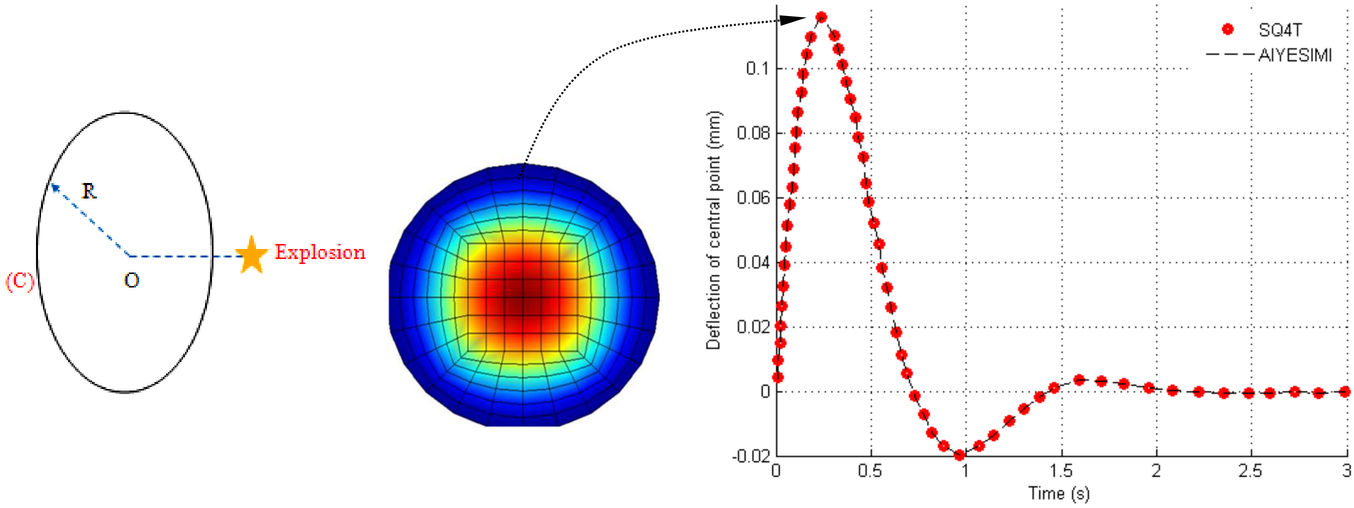

(a) (b)

Fig. 9. (a) The clamped (C) circular plate subjected to blast loading, (b) The vibration of this damped plate at central point.

3.4 A circular plate with clamped at circumference under blast loading

Finally, the clamped circular plate under blast loading is presented. The dimensions and material properties are shown as follow R = 2m, thickness thk = 0.003m, $E = 30x10^7$ kN/m^2, $\rho = 2778$ kg/m^3, $\nu = 0.3$ and in Figure 9a. The blast load parameters are taken as $p_{s\max} = 22.1804$ kN/m^2, $\gamma = 2$ and $T_s = 0.1$ by following [13]. The vibration of damped circular plate subject to blast loading is displayed in Figure 9b. Once again, the our result is in good agreement with the other from [13].

4. Conclusion

This paper presented the dynamic response of plate structures subjected to blast loading based on novel quadrilateral SQ4T elements. Due to the framework of the FSDT and the TIS, the SQ4T element becomes an efficient flat quadrilateral element for dynamic analysis. The results achieved in this study are shown in details and compared with other available numerical results to illustrate the robustness of these elements. The paper is limited to the scope of introducing an alternative approach to the problems related to blast loading and plate structures. The paper also helps designers to have a better understanding of behavior types of these structures under blast loading. In the future, the present element will be able to apply for analysis of various structures.

Conflict of Interest

The author declared no potential conflicts of interest with respect to the research, authorship and publication of this article.

Funding

The author received no financial support for the research, authorship and publication of this article.

References

[1] Brode, H.L., Numerical Solutions of Spherical Blast Waves. *Journal of Applied Physics*, 1955. 26(6): p. 766-775.
[2] PS, B., *Explosive loading of engineering structures*. E & FN Spon, London, 1997.
[3] Henrych, J., *The Dynamics of Explosion and Its Use*. Elsevier, Amsterdam, 1979.
[4] John H and P. S, *Blast and Ballistic Loading of structures*. Butterowrth-Heinemenn, Oxford, 1994.
[5] Nguyen, T.P. and M.T. Tran, Response of Vertical Wall Structures under Blast Loading by Dynamic Analysis. *Procedia Engineering*, 2011. 14: p. 3308-3316.
[6] Jacinto, A.C., R.D. Ambrosini, and R.F. Danesi, Experimental and computational analysis of plates under air blast loading. *International Journal of Impact Engineering*, 2001. 25(10): p. 927-947.
[7] Geretto, C., S. Chung Kim Yuen, and G.N. Nurick, An experimental study of the effects of degrees of confinement on the response of square mild steel plates subjected to blast loading. *International Journal of Impact Engineering*, 2015. 79: p. 32-44.
[8] Aune, V., et al., Experimental study on the response of thin aluminium and steel plates subjected to airblast loading. *International Journal of Impact Engineering*, 2016. 90: p. 106-121.
[9] Chung Kim Yuen, S., et al., The influence of orientation of blast loading on quadrangular plates. *Thin-Walled Structures*, 2018. 131: p. 827-837.
[10] Choi, J.-H., et al., Evaluation of blast resistance and failure behavior of prestressed concrete under blast loading. *Construction and Building Materials*, 2018. 173: p. 550-572.
[11] Badshah, E., et al., Review of Blast Loading Models, Masonry Response, and Mitigation. *Shock and Vibration*, 2017. 2017: p. 15.
[12] Tuna, M. and H.S. Turkmen, Dynamic Behavior of a Plate Under Air Blast Load Using Differential Quadrature Method. *ASME 2007 International Mechanical Engineering Congress and Exposition*, 2007. 42959: p. 221-228.
[13] Aiyesimi Y. M., A. A. Mohammed, and S. Sadiku, A Finite Element Analysis of the Dynamic Response of A Thick Uniform Elastic Circular Plate Subjected to an Exponential Blast Loading. *American Journal of Computational and Applied Mathematics*, 2011. 1(2): p. 57-62.
[14] Rabczuk, T., P.M.A. Areias, and T. Belytschko, A meshfree thin shell method for non-linear dynamic fracture. *International Journal for Numerical Methods in Engineering*, 2007. 72(5): p. 524-548.
[15] Rabczuk, T., et al., Immersed particle method for fluid–structure interaction. *International Journal for Numerical Methods in Engineering*, 2010. 81(1): p. 48-71.
[16] Rabczuk, T. and T. Belytschko, A three-dimensional large deformation meshfree method for arbitrary evolving cracks. *Computer Methods in Applied Mechanics and Engineering*, 2007. 196(29): p. 2777-2799.
[17] That-Hoang, L.T., et al., Enhancement to four-node quadrilateral plate elements by using cell-based smoothed strains and higher-order shear deformation theory for nonlinear analysis of composite structures. *Journal of Sandwich Structures & Materials*. 2020. 22(7): p. 2302-2329.
[18] Bui, T.Q., et al., On the high temperature mechanical behaviors analysis of heated functionally graded plates using FEM and a new third-order shear deformation plate theory. *Composites Part B: Engineering*, 2016. 92: p. 218-241.
[19] Nguyen-Van, H., et al. Nonlinear Static Bending Analysis of Functionally Graded Plates Using MISQ24 Elements with Drilling Rotations. *ACOME 2017: Proceedings of the International Conference on Advances in Computational Mechanics*, 2017. 461-475.
[20] Ton-That, H.L., H. Nguyen-Van, and T. Chau-Dinh, An Improved Four-Node Element for Analysis of Composite Plate/Shell Structures Based on Twice Interpolation Strategy. *International Journal of Computational Methods*, 2020. 17(6): p. 1950020.
[21] Ton That, H.L., H. Nguyen-Van, and T. Chau-Dinh, Nonlinear Bending Analysis of Functionally Graded Plates Using SQ4T Elements based on Twice Interpolation Strategy. *Journal of Applied and Computational Mechanics*, 2020. 6(1): p. 125-136.
[22] Ton-That, H.L., Improvement on eight-node quadrilateral element (IQ8) using twice-interpolation strategy for linear elastic fracture mechanics. *Engineering Solid Mechanics*, 2020. 8(4): p. 323-336.
[23] Reddy, J.N., *Theory and Analysis of Elastic Plates and Shells*. CRC Press, 2007.
[24] Zheng, C., et al., A novel twice-interpolation finite element method for solid mechanics problems. *Acta Mechanica Sinica*, 2010. 26(2): p. 265-278.
[25] Wu, S.C., et al., A twice-interpolation finite element method (TFEM) for crack propagation problems. *International Journal of Computational Methods*, 2012. 09(04): p. 1250055.
[26] Bui, T.Q., et al., A consecutive-interpolation quadrilateral element (CQ4): Formulation and applications. *Finite Elements in Analysis and Design*, 2014. 84: p. 14-31.
[27] Ferreira, A.J.M., *MATLAB Codes for Finite Element Analysis*. Springer, 2009.
[28] Nelson L., Priyan M., and T. Ngo, Response spectrum solutions for blast loading. *Electronic Journal of Structural Engineering*, 2004. 4(4): p. 28-44.

ORCID iD

Hoang Lan Ton-That https://orcid.org/0000-0002-3544-917X

How to cite this article: Ton-That H.L. A Novel Quadrilateral Element for Dynamic Response of Plate Structures Subjected to Blast Loading, *J. Appl. Comput. Mech.*, 6(SI), 2020, 1314–1323. https://doi.org/10.22055/JACM.2020.33959.2314